**Journal of Computational Methods in Molecular Design, 2015, 5 (3):69-78**

**Scholars Research Library**
*(http://scholarsresearchlibrary.com/archive.html)*

**ISSN : 2231- 3176**
**CODEN (USA): JCMMDA**

# Investigation of pyrrolidine hydrodenitrogenation modelling on theoretical catalysts sites under hydrogen pressure

**Simplice Koudjina, Urbain A. Kuevi, Y. Guy S. Atohoun, Gaston A. Kpotin, Alice M. T. Kpota Houngue and Jean-Baptiste Mensah***

*Laboratory of Theoretical Chemistry and Molecular Spectroscopy, Faculty of Sciences and Technic, University of Abomey-Calavi, Cotonou-Benin*

---

**ABSTRACT**

*The theoretical investigation of hydrotreatment of pyrrolidine without catalyst and with three catalysts of hydrotreating such as the tungsten disulfide, the zinc chloride and the aluminum chloride, was performed. The calculations were carried out by ab initio methods MP2 and DFT/B3LYP in 6-31G* and Lanl2DZ basis sets. The experimental conditions taken into account by the calculations were 40 bars and 523 K. The elimination of the heteroatom source under $NH_3$ form was modeled in two successive hydrogenolysis stages, which produced butan-1-amine and butane respectively. The lowest activation energy of the reaction was obtained with zinc chloride. The Infrared spectra calculated by TDHF/aug-cc-pVDZ method, for the various chemical systems, before and after their transformations, made it possible to propose a mechanism of reaction.*

**Keywords:** Pyrrolidine; Catalytic Hydrotreatment; Hydrogenolysis; TDHF, Activation Energy.

---

## INTRODUCTION

Hydrodenitrogenation is one of the most important of all the catalytic hydrotreatment cracking reactions. It is a reaction used to eliminate, under hydrogen pressure, the nitrogen content of molecules, which are then transformed into saturated or unsaturated hydrocarbons [1]. Taking into account the increasing requirements of the consumers as regards quality of the products, and taking into account the technological progress made in the field of the refining to have cheap products, the hydrodenitrogenation [2] grew up favourably thanks to the crisis of oil and the need for improving the heavy residues of crude oil [3]. The presence of high contents of non desired heteroatoms, particularly the nitrogen, in the products of refinery, led petrochemical industry to pay attention to their eliminations [4]. Indeed, industrially, nitrogened compounds are poisons for acid catalysts used in this kind of treatment. Moreover, the elimination of nitrogen makes it possible to obtain products of a better quality, offering a greater stability during storage [5].

The use of effective numerical methods (*ab initio* methods), for the study of the molecular reactivity in general or the hydrodenitrogenation reaction in particular, has a principal interest for chemistry. Indeed, approached under the angle of fundamental research in theoretical chemistry, the significant question of the improvement of the quality of the fuels opened new prospects with petrochemical industry [6,7].

The theoretical study of the catalytic hydrodenitrogenation of pyrrolidine realized in this present work is part of this framework. The Pyrrolidine or tetrahydropyrrole ($C_4H_9N$) is a liquid heterocyclic compound, colorless with a highly volatile amine odor (Figure 1). It is submitted to catalytic hydrotreating process in oil refineries to rid him of his heteroatom [8,9]. By the quantum chemistry methods (DFT and MP2) in 6-31G* [10] and Lanl2DZ [11,12] basis sets, the catalytic Hydrotreatment of pyrrolidine, under a hydrogen gas pressure of 40 bars and at the temperature of 523 K, has been simulated without catalyst [13,14] and with catalysts. The catalysts used in this study on which the

molecule has been adsorbed, are the Zinc Chloride ($ZnCl_2$) [15,16], the Aluminum Chloride ($AlCl_3$) [17] and the Tungsten Disulfide ($WS_2$) [18] modeled by a catalytic site with three anionic vacancies $WS_3H_3^+$ (Figure 1). On the one hand, the reaction without catalyst is made in the 6-31G* atomic orbital basis set, and on the other hand, the reactions with catalysts were performed in the Lanl2DZ basis set, which takes into account the heavy metal of catalysts. The aim of this study is centered on the elimination of the heteroatom source of the toxicity of pyrrolidine, which was modeled in two successive hydrogenolysis stages. The first stage has produced butan-1-amine and the second leads to the formation of ammoniac ($NH_3$) and butane ($C_4H_8$) molecules.

This paper is organized as follows: section 2 summarizes the theoretical and computational details; results are presented and discussed in section 3, whereas section 4 draws conclusions and outlook.

**Figure 1: Structure of Pyrrolidine and Hydrotreatment Catalysts optimized with B3LYP level of approximation in Lanl2DZ basis set**

## MATERIALS AND METHODS

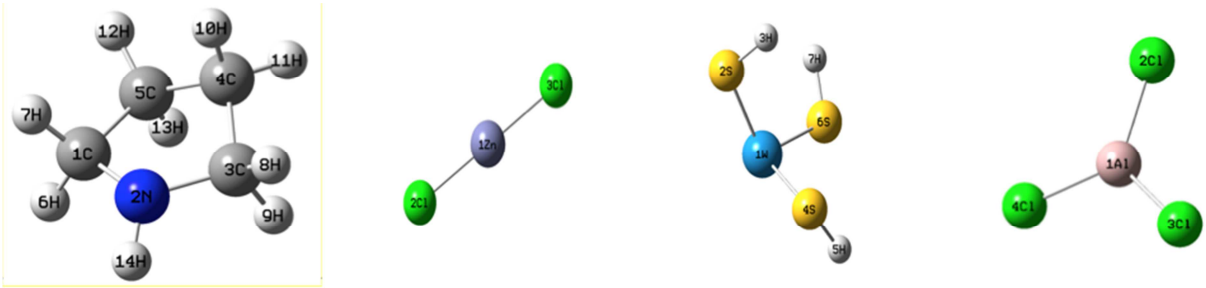


The calculations were carried out by the methods DFT/B3LYP and MP2 in the 6-31G* and Lanl2DZ basis sets, which takes into account the heavy metal in the catalyst systems and using the program Gaussian09-D01 [19] that is implemented by the drafting package ChemDraw Ultra 10.0 [20] and Gaussview5.0.8. [21]. They are calculations of geometric parameters of initial, final and transition states (*TS*) of different studied chemical transformations, IRC (Intrinsic Reaction Coordinates) paths and thermodynamic and kinetic parameters such as reaction energies ($\Delta E$), activation energies (*Ea*) at the experimental conditions at temperature of 523 K and pressure of 40 bars [13]. The transition states are determined by the *TS Berny* methods. The energetic variation curve has been determined with IRC. Three steps modeled the reactions.

- Adsorption of the reactive molecule on the catalyst surface, simulated by its approach of the catalyst surface until the energy minimization of all of the chemical system. In that state the adsorption is supposed really performed (Figure 2). The reaction parameter controlled during this simulation stage is the distance between the nitrogen atom of the Pyrrolidine molecule and the metal atom of the catalyst surface (N-$M_{catalyst}$).
- Hydrogenolysis of first N-C bond (Figure 3)
- Hydrogenolysis of second N-C bond (Figure 4).

The first of those reaction stages doesn't concern the reaction performed without catalyst. For each of hydrogenolysis, the transition state (*TS*) of the reaction was first calculated by Berny algorithm, before the calculation of Intrinsic Reaction Coordinates (*IRC*) paths. The reaction parameters controlled during these simulation stages are the N-C distances in the adsorbed molecule (Figures 3 and 4).

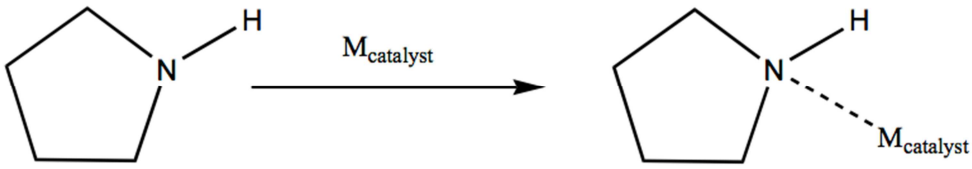


**Figure 2: Scheme of adsorption of the Pyrrolidine molecule on the catalysts**

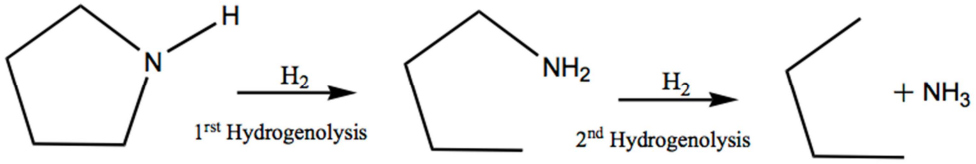


**Figure 3: Scheme of hydrogenolysis of the Pyrrolidine molecule without catalyst**

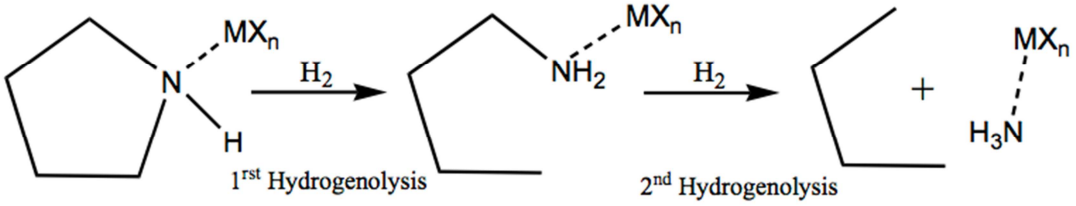


**Figure 4: Scheme of hydrogenolysis of the Pyrrolidine molecule adsorbed on catalysts ($MX_n$ = $ZnCl_2$, $WS_2$, $AlCl_3$)**

## RESULTS AND DISCUSSION

***Geometric parameters of Pyrrolidine***

The optimized geometric parameters of the Pyrrolidine molecule calculated in Lanl2dz basis set, with the MP2 and DFT/B3LYP methods are consigned in the table 1. The experimental data given in the same table were provided by the Cambridge Crystallography DATA Center (CCDC) [22]. The figure 1 shows it's drawing with the labels of atoms.

**Table 1: Geometric optimized parameters of pyrrolidine**

| | Distances (Å) | | | | Angles (°) | | | | Torsion (°) | | |
|---|---|---|---|---|---|---|---|---|---|---|---|
| | *MP2* | *DFT* | *Exp* | | *MP2* | *DFT* | *Exp* | | *MP2* | *DFT* | *Exp* |
| $N^2C^1$ | 1.50 | 1.49 | 1.51 | $N^2C^3C^4$ | 102.50 | 102.80 | 105.44 | $N^2C^3C^4C^5$ | -24.32 | -37.86 | -26.21 |
| $N^2C^3$ | 1.50 | 1.48 | 1.49 | $C^5C^1N^2$ | 102.50 | 104.83 | 105.06 | $C^3C^4C^5C^1$ | -0.03 | 36.51 | 31.93 |
| $C^3C^4$ | 1.57 | 1.54 | 1.48 | $C^3C^4C^5$ | 105.18 | 102.72 | 107.40 | $C^4C^5C^1N^2$ | 24.36 | -21.30 | -24.90 |
| $C^4C^5$ | 1.59 | 1.55 | 1.45 | $C^4C^5C^1$ | 105.18 | 103.59 | 104.68 | $C^5C^1N^2C^3$ | -41.74 | -2.65 | 9.18 |
| $C^5C^1$ | 1.57 | 1.55 | 1.52 | $C^1N^2C^3$ | 106.60 | 110.75 | 107.40 | $C^1N^2C^3C^4$ | 41.72 | 25.54 | 9.63 |
| $N^2H^{14}$ | 1.03 | 1.02 | 1.08 | $C^1N^2H^{14}$ | 115.12 | 115.88 | 118.50 | $C^1N^2C^3H^8$ | 161.66 | 145.64 | 129.05 |
| $C^3H^8$ | 1.10 | 1.09 | 1.08 | $C^3N^2H^{14}$ | 115.12 | 115.97 | 118.50 | $C^5C^1N^2H^{14}$ | -170.72 | -137.43 | -167.86 |
| $C^3H^9$ | 1.12 | 1.10 | 1.08 | $N^2C^1H^7$ | 110.32 | 110.34 | 110.48 | $C^4C^3N^2H^{14}$ | 170.71 | 160.27 | 167.85 |
| $C^1H^6$ | 1.12 | 1.10 | 1.08 | $N^2C^3H^8$ | 110.32 | 111.21 | 110.48 | | | | |
| $C^1H^7$ | 1.10 | 1.09 | 1.08 | | | | | | | | |

The results of both calculation methods have been very close of the experimental values of literature given by the Cambridge Crystallography DATA Bases. But, the results of MP2 calculations have especially respected better the symmetry of the molecule.

***Hydrogenolysis of pyrrolidine without catalyst***

Firstly, the pyrrolidine $N^2$-$C^1$ bond has undergone a hydrogenolysis [23] without catalyst, under the reaction conditions of 523 K and 40 bars. The hydrogenolysis simulation was performed by approach of one hydrogen molecule ($H^{15}$-$H^{16}$) towards this bond, until its rupture and opening of the molecule ring. In this reaction stage, the MP2 interatomic distances $N^2C^1$ and $H^{15}H^{16}$ are passed from 1.51 Å and 0.74 Å to 2.91 Å and 2.59 Å respectively (Table 2). These important increasing of interatomic distances mean that the corresponding bonds were broken. In addition, the interatomic distances $N^2H^{15}$ and $C^1H^{16}$ are passed from 2.72 Å and 3.72 Å to 1.02 Å and 1.10 Å respectively (Table 2). Then the corresponding bonds were established.

The Mulliken atomic charges of $N^2$ and $C^1$ atoms were calculated and the corresponding values are passed respectively from -0.582 ua and -0.206 ua at the beginning, to -0.734 ua and -0.196 ua at the transition state. Also, Mulliken atomic charges of $H^{15}$ and $H^{16}$ atoms of the hydrogen molecule are passed from 0.055 ua and -0.058 ua, to 0.329 ua and -0.424 ua respectively. During these variations, the electronic charges of the $N^2$ and $H^{16}$ atoms have increased while those of $C^1$ and $H^{15}$ atoms have decreased. Thus, the $N^2$-$C^1$ and $H^{15}$-$H^{16}$ bonds have probably undergone heterolytic ruptures before the formation of $N^2$-$H^{15}$ and $C^1$-$H^{16}$ new bonds.

**Table 2: Variation of geometric parameters of complex [Pyrrolidine-$H_2$], during the 1$^{rst}$ and 2$^{nd}$ hydrogenolysis, at the main stages of the process**

| Distances (Å) | Initial State | | Transition State | | Final State | | Standard Values (Å) | Observations |
|---|---|---|---|---|---|---|---|---|
| | DFT | MP2 | DFT | MP2 | DFT | MP2 | | |
| $H^{15}$-$H^{16}$ | 0.75 | 0.74 | 1.37 | 1.40 | 2.62 | 2.59 | 0.73 (H-H) | Rupture |
| $H^{17}$-$H^{18}$ | 0.75 | 0.74 | 1.31 | 1.34 | 2.15 | 2.31 | 0.73 | Rupture |
| $C^{1}$-$H^{16}$ | 3.67 | 3.72 | 2.18 | 2.02 | 1.10 | 1.10 | 1.09 (C-H) | Formation |
| $C^{3}$-$H^{18}$ | 3.61 | 3.57 | 2.14 | 2.00 | 1.10 | 1.10 | 1.09 | Formation |
| $N^{2}$-$H^{17}$ | 2.50 | 2.53 | 1.08 | 1.08 | 1.01 | 1.02 | 1.01 (N-H) | Formation |
| $N^{2}$-$H^{15}$ | 2.64 | 2.72 | 1.07 | 1.07 | 1.02 | 1.02 | 1.01 | Formation |
| $N^{2}$-$C^{1}$ | 1.49 | 1.51 | 2.14 | 2.03 | 2.97 | 2.91 | 1.48 (C-N) | Rupture |
| $N^{2}$-$C^{3}$ | 1.48 | 1.51 | 2.16 | 2.04 | 3.09 | 2.97 | 1.48 | Rupture |

The vibrational IR spectra [24] calculated under incident wavelength of 532 nm in both initial and final sates are shown on the figure 5. In the initial state spectrum (Figure 5a), belonging to the region 1250-1020cm$^{-1}$, one observes a peak characteristic of amine C-N bond [25], at the frequencies of 1144.8cm$^{-1}$. In the final state (Figure 5b), the same peak appears at the frequency of 1153.7cm$^{-1}$. This means that both pyrrolidine and reaction product always contain the C-N bond. But, the comparison of the peaks intensities shows a highest intensity in initial state. The rupture of the first C-N bond in the final product can explain that.

**Figure 5: IR spectra in initial state (a) and final state (b)**

These different spectra show the variation of the vibrational frequencies during the 1$^{rst}$ hydrogenolysis. The vibrational normal coordinates have been evaluated at the B3LYP/6-31G* level whereas the polarizabilities and their geometrical derivatives at the TDHF/aug-cc-pVDZ level [26]. Each transition is represented by a Lorentzian function with FWHM (Full Width Half Maximum) of 10 cm$^{-1}$ and a multiplicative factor of 0.96 was used to scale the vibrational frequencies at the simulation of the harmonic frequencies. The same analysis is obtained with the IR spectra, which have been done in the 2$^{nd}$ hydrogenolysis.

The product obtained at the end of this first chemical transformation was thus a primary amine: butan-1-amine (Figure 6).

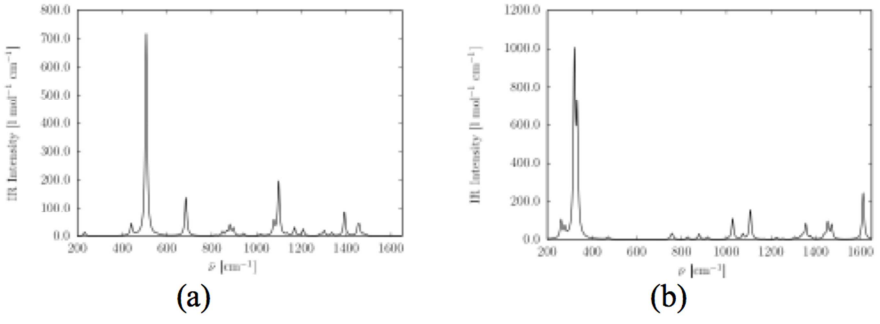

**Figure 6a: Stages of the 1$^{rst}$ hydrogenolysis without catalysts under the hydrogen pressure of 40bars at the temperature of 523K**

Secondly, for the simulation of following hydrogenolysis (Figure 6b), another hydrogen molecule ($H^{17}$-$H^{18}$) was then approached towards the $N^{2}$-$C^{3}$ bond of the primary amine molecule given by the first hydrogenolysis of pyrrolidine molecule. During this reaction stage, the interatomic distances $N^{2}$-$C^{3}$ and $H^{17}$-$H^{18}$ were also broken (Figure. 6b) and the interatomic distances $N^{2}$-$H^{17}$ and $C^{3}$-$H^{18}$ were established, like firstly (Table 2).

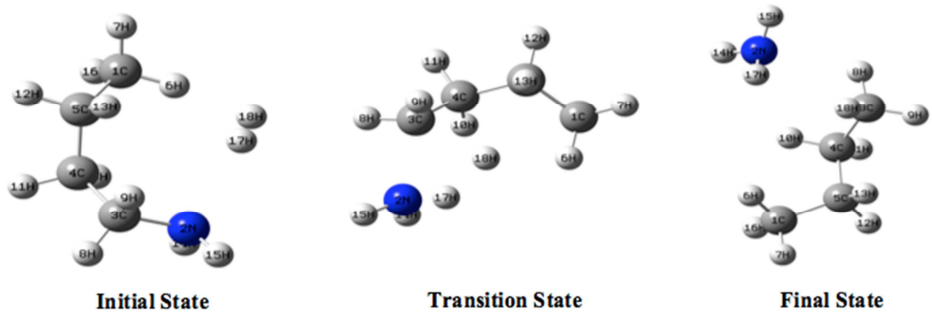


**Figure 6b: Stages of the 2nd hydrogenolysis without catalysts under the hydrogen pressure of 40bars at the temperature of 523K**

From beginning to the transition state of second hydrogenolysis, the Mulliken atomic charges of $N^2$ and $C^3$ are varied respectively from -0.745 u.a and -0.195 u.a to -0.889u.a and -0.181u.a. Also, those of $H^{17}$ and $H^{18}$ are passed from 0.264 u.a and -0.303 u.a to 0.295 u.a and 0.163 u.a, respectively. In this case the hydrogenolysis was also performed by heterolytic ruptures of $N^2$-$C^3$ and $H^{17}$-$H^{18}$ bonds. The $N^2$-$H^{17}$ and $C^3$-$H^{18}$ new bonds were established too. The reaction products were butane and ammonia molecules.

The calculations of IRC paths of both hydrogenolysis of pyrrolidine molecule without catalyst, have allowed calculating their activation energy ($E_a$) and the reaction energy ($\Delta E$). The calculated values of these parameters are consigned in the Table 3.

**Table 3: Activation Energy and the reaction energy of Hydrodenitrogenation of pyrrolidine molecule without catalyst**

| Reaction Stages | MP2 | | B3LYP | |
|---|---|---|---|---|
| | $E_a$ | $\Delta E$ | $E_a$ | $\Delta E$ |
| 1rst hydrogenolysis | 100 | -30 | 90 | -20 |
| 2nd hydrogenolysis | 98 | -20 | 88 | -25 |

These results make it possible to note that the first hydrogenolysis was the limiting stage of the whole of the reaction ($E_{a1} > E_{a2}$); both stages of the reaction were exoenergetic ($\Delta E_1 < 0$ and $\Delta E_2 < 0$).

***Adsorption of Pyrrolidine on catalyst surface.***

The molecule was approached of each catalyst and the geometry of the chemical system [Molecule-Catalyst] obtained was optimized with a minimum of energy. The interatomic distances $N^2$-$M^{15}$ (M = Zn, W and Al) of the system are the geometrical controlled parameters. The main geometrical parameters calculated at the adsorption [27], by the B3LYP and MP2 levels of approximation, in the Lanl2dz basis set, are consigned in table 4. The figure 7 shows the drawing of pyrrolidine molecule adsorbed on the surface of each catalyst.

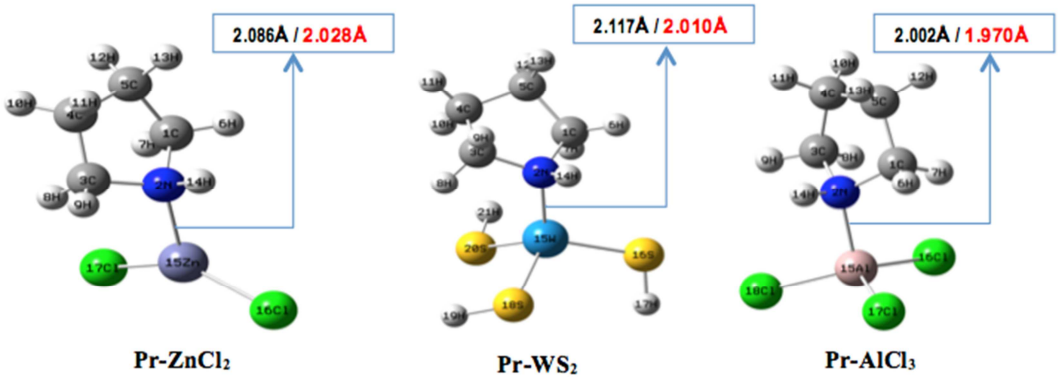


**Figure 7: Drawings of the pyrrolidine molecule adsorbed on the catalyst surfaces. The black values of $N^2$-$M^{15}$ adsorption distance are the calculated values and the red one are the standard values in the crystallographic database**

**Table 4: Main geometrical parameters calculated at the adsorption**

| | MP2 | | | DFT | | |
|---|---|---|---|---|---|---|
| | M = Zn | M = W | M = Al | M = Zn | M = W | M = Al |
| *Distances (Å)* | | | | | | |
| $N^2$-$M^{15}$ | 2.09 | 2.12 | 2.00 | 2.10 | 2.10 | 1.99 |
| $N^2C^1$ | 1.54 | 1.56 | 1.56 | 1.52 | 1.55 | 1.53 |
| $N^2H^{14}$ | 1.03 | 1.03 | 1.03 | 1.03 | 1.03 | 1.03 |
| *Angles (°)* | | | | | | |
| $C^1N^2C^3$ | 104.29 | 108.04 | 107.19 | 103.78 | 107.35 | 103.75 |
| $N^2C^3C^4$ | 104.68 | 103.77 | 105.19 | 105.55 | 104.59 | 104.98 |
| $C^5C^1N^2$ | 106.19 | 105.18 | 104.44 | 105.55 | 105.27 | 104.97 |

On the whole, the values of the geometrical parameters of the molecule haven't varied much at the adsorption. However, one observes a slight increase of the $N^2$-$C^1$ and $N^2$-$C^3$ interatomic distances. For the MP2 calculations, for example, they pass respectively from 1.50 Å to 1.56 Å, on the $WS_2$ catalyst. The same tendency is observed for both MP2 and B3LYP methods and all catalysts (Tables 1 and 2). The C-N chemical bonds thus are slightly stretched and weakened in the adsorbed molecule compared with the lonely molecule. This weakening of these bonds could support their rupture in the continuation of the reaction process at the hydrogenolysis of these bonds. Also, at the adsorption, the value of $C^1N^2C^3$ angle was increased from 106.60° to 108.04° and 107.19°, on the $WS_2$ and $AlCl_3$ catalysts respectively. But, it is decreased to 104.29° in the case of $ZnCl_2$ catalyst (Tables 1 and 2). These results mean that at the adsorption, the pyrrolidine molecule is more damped on the surface of the first two catalysts than on the surface of $ZnCl_2$. In addition, the distances $N^2$-$M^{15}$ (M = Zn, W and Al) between the metal atoms of catalysts and the nitrogen atom of the molecule ring are 2.086Å, 2.177Å and 2.002Å respectively and compared with the N-M distances of the molecule ring 2.028Å, 2.010Å and 1.970Å in the crystallographic data. These bond lengths are substantially in accordance with the experimental data provided in the literature [28]. The adsorption enthalpies ($\Delta H_{ads}$) and the vibrational energies ($\Delta\nu$) of pyrrolidine are also calculated for each case and recorded in the Table 5.

**Table 5: Adsorption enthalpies ($\Delta H_{ads}$) and the vibrational energies ($\Delta\nu$) of pyrrolidine**

| Adsorbed systems | *ΔHads* (kJ/mol) | | *Δν* (kJ/mol) | |
|---|---|---|---|---|
| | DFT | MP2 | DFT | MP2 |
| Pyrrolidine-$ZnCl_2$ | -308.03 | -304.73 | 355.80 | 355.91 |
| Pyrrolidine-$WS_2$ | -312.11 | -310.03 | 421.31 | 423.10 |
| Pyrrolidine-$AlCl_3$ | -259.47 | -257.79 | 364.77 | 365.28 |

These results above have shown that all the three adsorptions were chemisorptions and not physisorptions, because the values of the calculated adsorption enthalpies lie between -40 and -800 kJ/mol [27]. The $N^2$-$M^{15}$ bonds were thus established at the adsorption. The lowest absolute values of adsorption enthalpies ($|\Delta Hads|$) were given by the MP2 calculations (Table 5).

At the contact between a molecule and the catalyst surface, thermal energy produced by the impact is partly absorbed by catalyst, so that the molecule does not rebound and does not move away from the surface of catalyst. The remainder of this thermal energy is converted into vibration energy for the system [Molecule-Catalyst]. The speed of adsorption of a molecule on the surface of a catalyst depend thus on the capacity on this last to absorb this thermal energy [28].

The high values of vibration energy ($\Delta\nu$) of the pyrrolidine molecule on catalysts have shown that the molecule has undergone strong vibrations after adsorption on catalysts surfaces. This situation could cause the weakening of molecule C-N bonds and could favor their hydrogenolysis. Thus, at the adsorption the pyrrolidine molecule was attached on each catalyst surface with formation of $N^2$-$M^{15}$ bond.

The whole of above results (geometrical and energy parameters) shown that the pyrrolidine is chemically absorbed on the catalysts without many transformations of its geometry and symmetry.

***Hydrogenolysis of pyrrolidine in presence of catalysts***

The simulation of denitrogenation of pyrrolidine molecule was performed in presence of three catalysts: $ZnCl_2$, $WS_2$ and $AlCl_3$. The N-C bonds of the molecule are successively undergone to the first and the second hydrogenolysis after its adsorption on the catalysts surfaces. The transition states of both transformations were calculated by the Berny algorithm. The figures 8 and 9 show the drawings of different stages of the 1$^{rst}$ hydrogenolysis and the 2$^{nd}$ hydrogenolysis in presence of catalysts.

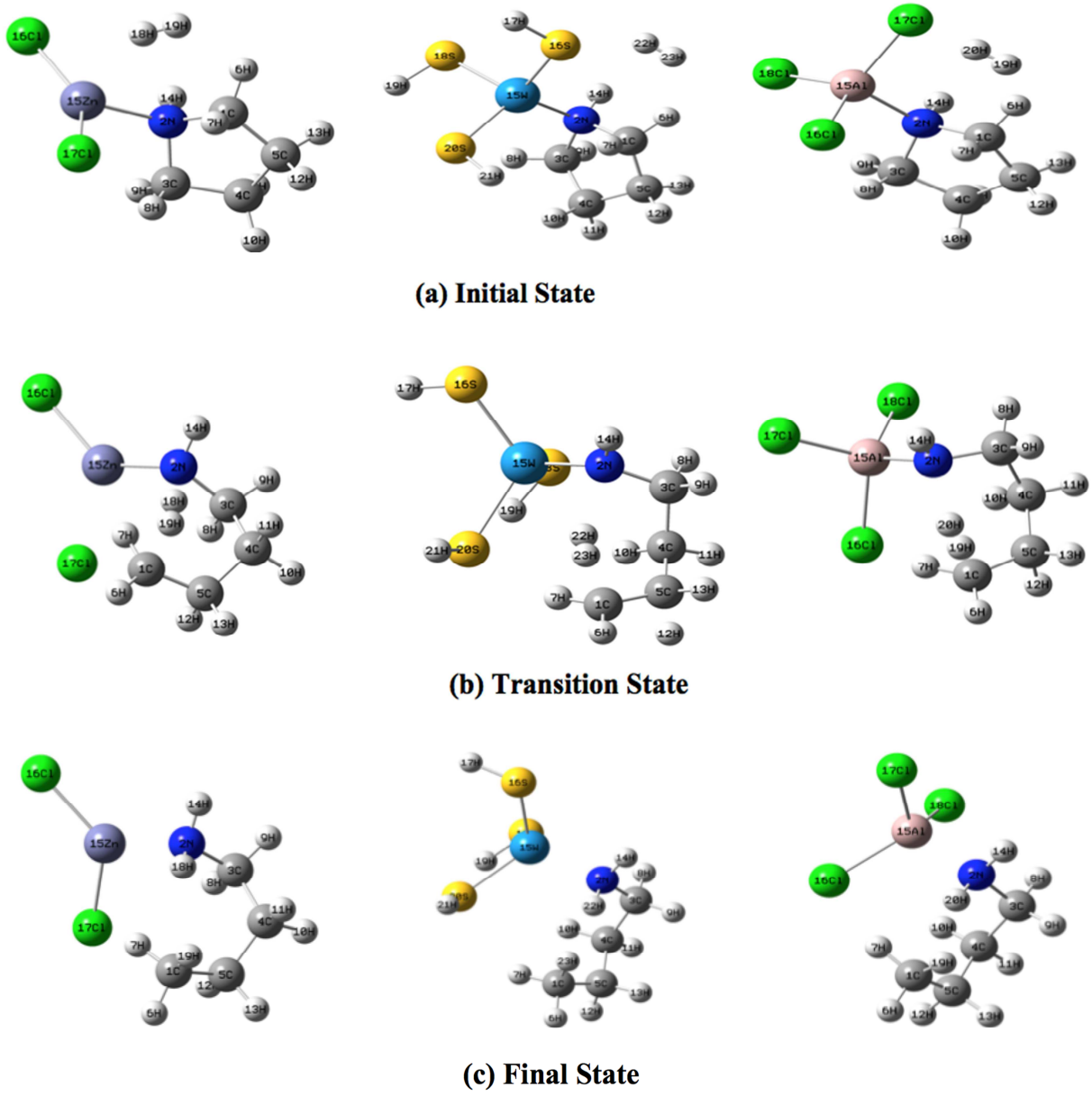


**Figure 8: Drawings of system [Molecule-$H_2$] at main stages of the 1$^{rst}$ hydrogenolysis of Pyrrolidine in presence of catalysts**

In the presence of catalysts, the first hydrogenolysis has also leaded to butan-1-amine as intermediate product (Figure 8c). The opening of the molecular ring has followed the rupture of the $N^2$-$C^1$ bond and has allowed the fixation of both hydrogen atoms of the hydrogen molecule on the $N^2$ and $C^1$ atoms of pyrrolidine. So, the new chemical bonds N-H and C-H were established. Like in the case of the reaction without catalyst, the products obtained at the end of the second hydrogenolysis were also butane and ammonia, except for the reaction performed in presence of $AlCl_3$**.** For this latter case, an atom of the approached hydrogen molecule has rather migrated towards catalyst, to bind oneself to a chlorine atom, instead to the group $NH_2$ of butan-1-amine (Figure 9). A subsequent treatment at high temperature of the final product obtained will allow the recovery of ammonia and regeneration of the catalyst [29,30].

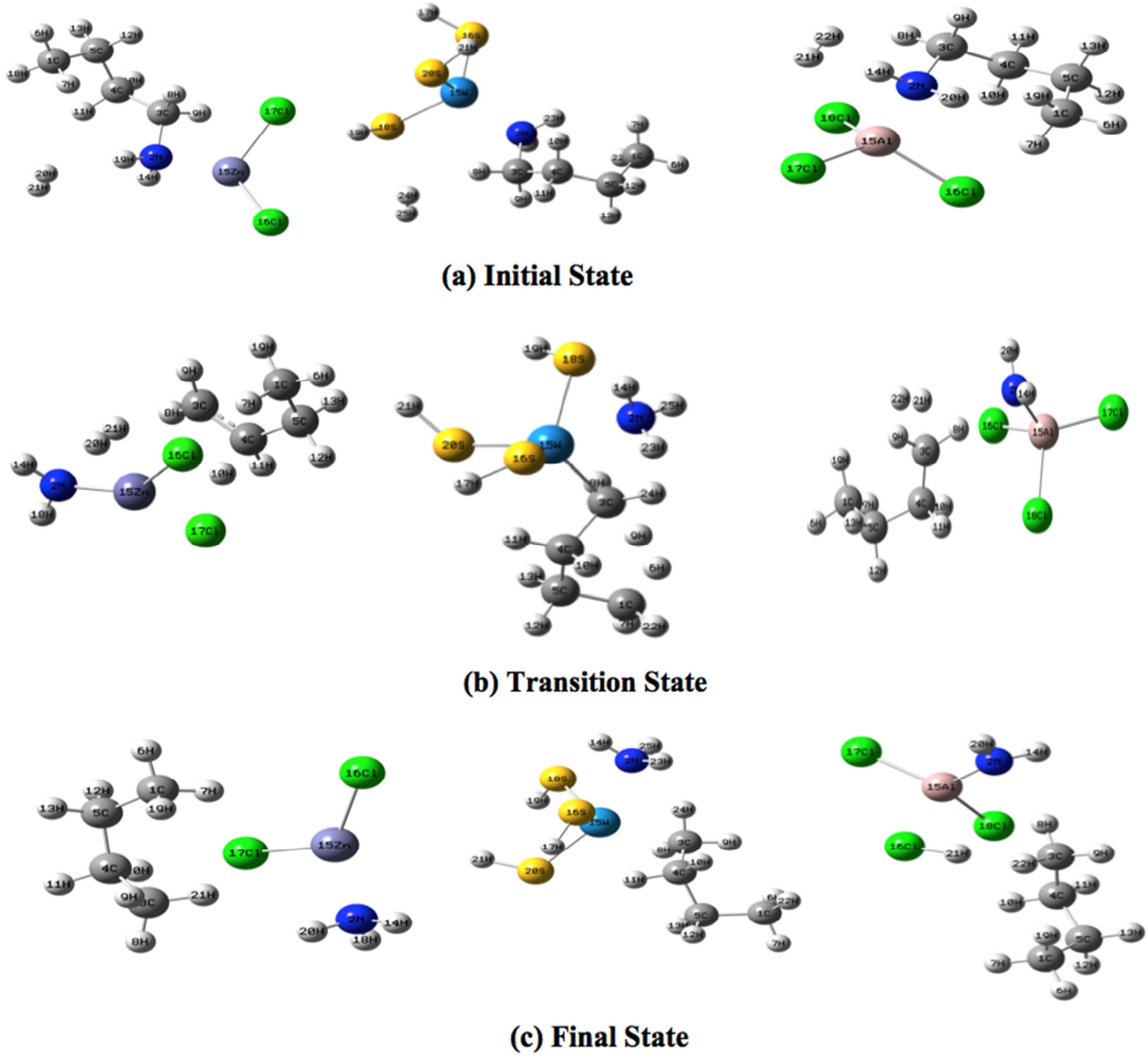


**Figure 9: Reaction enthalpies (*ΔH*), vibrational energies (*Δv*), Gibbs energies (*ΔG*) and activation energies of 1st and 2nd hydrogenolysis of pyrrolidine**

Concerning the Mulliken electronic charges analysis, the same observations are made, like in the previous case of reaction without catalyst. On the all of the three catalysts, the bond ruptures were heterolytic. The table 6 shows the reaction enthalpies (*ΔH*), the vibrational energies (*Δv*), the Gibbs energies (*ΔG*) and the activation energies of 1st and 2nd hydrogenolysis (HDL) of pyrrolidine.

**Table 6: Reaction enthalpies (*ΔH*), vibrational energies (*Δv*), Gibbs energies (*ΔG*) and activation energies of 1st and 2nd hydrogenolysis of pyrrolidine**

| Catalysts | *ΔH* ($10^3$.kCal.mol$^{-1}$) | | *Δv* (kJ.mol$^{-1}$) | | *ΔG* ($10^3$.kCal.mol$^{-1}$) | | $E_a$ (kCal.mol$^{-1}$) | |
|---|---|---|---|---|---|---|---|---|
| | 1rst HDL | 2nd HDL | 1rst HDL | 2nd HDL | 1rst HDL | 2nd HDL | 1rst HDL | 2nd HDL |
| $ZnCl_2$ | -191.83 | -192.57 | 381.20 | 427.67 | -191.90 | -192.66 | 35 | 13 |
| $AlCl_3$ | -162.38 | -163.12 | 388.46 | 438.42 | -162.46 | -163.20 | 30 | 16 |
| $WS_2$ | -195.19 | -196.69 | 444.64 | 514.22 | -195.28 | -196.78 | 20 | 27 |
| Without Catalyst | -133.92 | -134.67 | 371.43 | 421.96 | -133.97 | -134.72 | 88 | 112 |

In the three cases, the vibrational energies of the 2nd HGL were the highest. The molecule will have a higher vibration on the catalysts surface and that will be more favorable to the rupture of the targeted N-C bond. The catalyst $WS_2$ seems be the most kinetically indicated for the 1rst HGL because of the weakest value of $E_a$ (20 kCal.mol$^{-1}$), while $ZnCl_2$ would be more indicated to the 2nd HGL ($E_a$ = 13 kCal.mol$^{-1}$). In the all cases, the highest values of activation energies were obtained for the reaction without catalyst (88 and 112 kCal.mol$^{-1}$). The reaction

has been then easier with catalyst than without catalyst. In experiments, as far as possible, may be, it would be interesting to subject the molecule to the joint action of two catalysts $WS_2$ and $ZnCl_2$ to optimize the denitrogenation of pyrrolidine. The negative values of reaction enthalpies and Gibbs energies mean that, in the all cases, the both HGL are exoenergetic and thermodynamically favorable, respectively. On the basis of all of the results obtained, a probable mechanism has been proposed for the reaction (Figure 10).

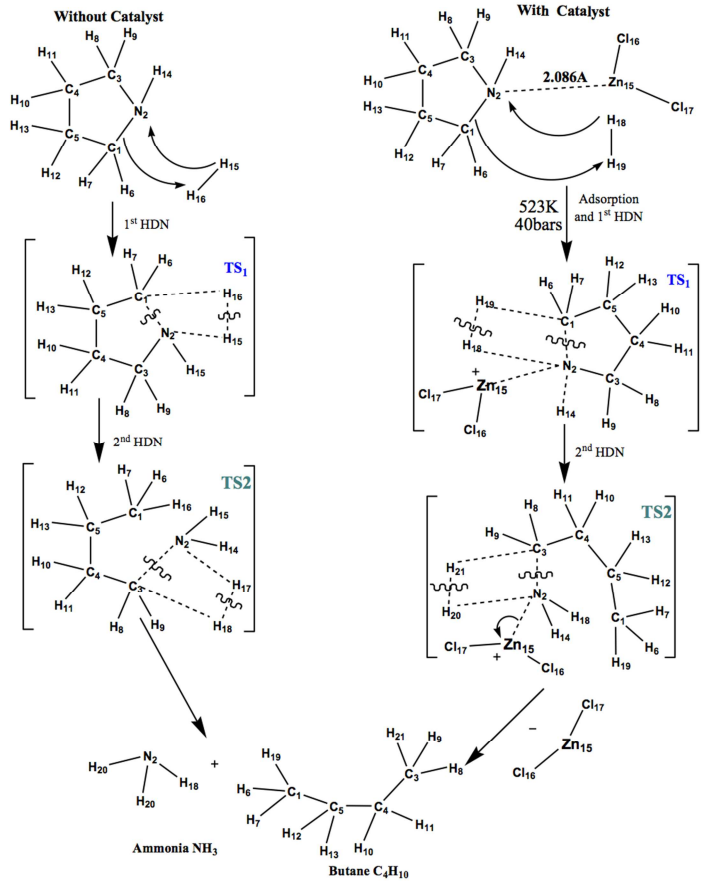


**Figure 10: Probable mechanisms of pyrrolidine Hydrodenitrogenation without and with catalyst**

## CONCLUSION

On basis of the numerical methods of chemistry, the theoretical investigation of hydrodenitrogenation of pyrrolidine had been performed without catalyst and in the presence of three catalysts hydrotreating. The calculations results shown that, subjected to such a treatment, the pyrrolidine molecule has leaded to the formation of the butane and the ammoniac molecules. The reaction passes by the formation of butan-1-amine as intermediate product, after the first hydrogenolysis. At the end of the whole of the reactions the catalysts have been good regenerated, according to the experimental results consigned in literature. This hydrotreating is thermodynamically more favorable and more advantageous in the presence of catalysts, because the reactions activation energies were lower with catalysts than without catalyst (Tables 5 and 6). Also, it would be interesting to subject the molecule to the joint action of both catalysts $WS_2$ and $ZnCl_2$ to optimize the denitrogenation of pyrrolidine. This will therefore be very advantageous for the heterolytic rupture of C-N bonds, which occur into this chemical system.

**Acknowledgments**
The calculations have been performed on the LACTHESMO Equipments of Professor Jean-Baptiste Mensah at the University of Abomey-Calavi (UAC-Benin) with the collaborations of the LCT/CECI at the University of Namur (Belgium) and of Department of Chemistry, at the Rutgers University (Camden, New Jersey, USA). We thank especially the Professors B. Champagne and L. A. Burke, who are our main partners in these fruitful collaborations with the previous universities respectively.

## REFERENCES

[1] X. Li, M. Lu, A. Wang, C. Song, Y. Hu, *J. Phys. Chem. C.*, **2008,** 112, 42**.**

[2] S. Li, J. Sung Lee, T. Hyeon, K. S. Suslick, *Applied Catalysis A: General*, 184, **1999**, 1-9
[3] D. D. Whitehurst, T. Isoda, I. Mochida, *Adv. Catal*., **1998,** 42, 345**.**
[4] J. Joffre, D. A. Lerner, P. Gneste, *Bull. Soc. Chim*. Belg., **1984,** 93, 831.
[5] I. V. Babich, *J. A. Fuel*, **2003,** 8, 607.
[6] S. Cristol, J-F Paul, C. Schovsbo, E. Veilly, E. Payen, *J. Catal.* **2006,** 239, 145–153.
[7] C. A. Badari, F. Lónyi, E. Drotár, A. Kaszonyi, J. Valyon, *Applied Catalysis B: Environmental*, 164, **2015**, 48-60.
[8] Satterfield, C. N., *Heterogeneous Catalysis in Industrial Practice*, McGraw-Hill, New York, **1991,** 339, 417.
[9] W. H. J. Stock, *Stud. Surf. Sci. Catal*. **1997,** 106, 41.
[10] W. J. Hehre, R. Ditchfield, J. A. Pople, *J Chem Phys*, **1972,** 56, 2257.
[11] D. E. Woon, T. H. Dunning, *J. Chem. Phys*, **1994,** 100, 2975.
[12] P. J. Hay, W. R. Wadt, *J. Chem. Phys*. **1985,** 82, 270.
[13] C. N. Satterfield, *Heterogeneous Catalysis in Industrial Practice*, **1991,** pp 339-417, McGraw Hill, New York.
[14] V. K. Smirnov, K. N. Irisova, Y. L. Kraev, E. L. Talisman, B. B. Zharkov, *Determination of Catalyst Activity in Hydrotreating*, Chem. Tech. Fuels Oil, **2011**.
[15] D. P. Mobley, A. T. Bell, *J. Catal*. **1980,** 64, 494-6.
[16] V. A. Robinovitch, Z. Y. Havin, *Kratkü Himitcheskü Spravotchnik*, Ed. Himiya. Leningrad, **1991.**
[17] T. Cai, M. He, *Catalysis Letters*, **2003,** 86, 1-3.
[18] J. Espino, L. Alvarez, C. Ornelas, J. L. Rico, S. Fuentes, G. Berhault, G. Alonso, *Catalysis Letters*, **2003,** 90, 1-2.
[19] M. J. Frisch, G. W. Trucks, H. B. Schlegel, G. E. Scuseria, M. A. Robb, J. R. Cheeseman, G. Scalmani, V. Barone, B. Mennucci, G. A. Petersson, et *al*. *Gaussian09, Revision D01*; Gaussian, Inc.: Wallingford, CT, **2013**.
[20] Z. Li, H. Wan, Y. Shi, P. Ouyang, *J. Chem. Inf. Comput.* Sci., **2004,** 44, 5.
[21] C. Peng, H. B. Schlegel, *Israel J. Chem*., **1994,** 33, 449.
[22] A. Parkin, I. D. H. Oswald, S. Parsons, *Acta Crystallogr*., Sect.B:Struct.Sci., **2004,** 60, 219.
[23] F. Jensen, *Introduction to computational chemistry*, 1st *ed. John Wiley*, New York, **1999**.
[24] E. B. Wilson, Jr, J. C. Decius, P. C. Cross, *Molecular Vibrations*: The Theory of Infrared and Raman Vibrational Spectra, Dover Publications, Mc Graw-Hill, New York, **1980**.
[25] R. M. Silverstein, F. X. Webster, D. J. Kiemle, *Spectrometric Identification of organic compounds*, 7th Edt, State University of New York, John Wiley & Sons, Inc, **2005**.
[26] O. Quinet, B. Champagne, *J. Chem. Phys*, **2002,** 117, 6.
[27] N. Ira Levine., *Physical Chemistry*, Third Edition, Chemistry Departement Brooklyn College City University of New York, **1988**.
[28] P. Atkins, J. De Paula, *Chimie Physique*, 8è éd., Edition De Boeck Université, **2008**.
[29] R. A. Sanchez-Delgado, *Organometallic Modeling of the HDS and HDN Reactions*, Kluwer Academic, **2002**.
[30] R. M. Silverstein, F. X. Webster, D. J. Kiemle, *Spectrometric Identification of organic compounds*, 7th Edt, State University of New York, John Wiley & Sons, Inc, **2005**.